Electronic supplementary information for:

Development of a new benzo(1,2-*b*:4,5-*b'*)dithiophene-based copolymer with conjugated (dithienylbenzothiadiazole)-vinylene side chains for efficient solar cells

Zhaojie Gu,[a] Ping Shen,*[a] Sai-Wing Tsang,[b] Ye Tao,[b] Peng Tang,[a] Yujuan Nie,[a] Bin Zhao[a] and Songting Tan*[a]

[a] *College of Chemistry, and Key Laboratory of Advanced Functional Polymeric Materials, College of Hunan Province, Key Laboratory of Environmentally Friendly Chemistry and Applications of Ministry of Education, Xiangtan University, Xiangtan 411105, P. R. China*

[b] *Institute for Microstructural Sciences, National Research Council of Canada, 1200 Montreal Road, Ottawa, Ontario, Canada K1A 0R6*

To whom correspondence should be addressed. E-mail: tanst2008@163.com; shenping802002@163.com

S1. Materials and Characterization

All the chemicals were purchased from Alfa Aesar and Shanghai Medical Company (China). THF and toluene were distilled from sodium/benzophenone prior to use. All other solvents and chemicals used in this work were analytical grade and used without further purification. All chromatographic separations were carried out on silica gel (200-300 mesh).

The ^{1}H NMR spectra were measured with Bruker AVANCE 400 spectrometer. UV-visible absorption spectra were measured on a Perkin-Elmer Lamada 25 UV/vis/NIR spectrometer. The photoluminescence emission spectra (EL) were recorded with Perkin-Elmer LS-50 luminescence spectrometer. The elemental analysis of the monomers and polymer were performed with an Elementar Vario EL III element analyzer for C, H, N and S determination. The average molecular weight and polydispersity index (PDI) of the copolymers were determined using Waters1515 gel permeation chromatography (GPC) analysis with THF as eluent and polystyrene as standard. Thermogravimetric analysis (TGA) measurement was conducted with a Netzsch TG 209 analyzer under nitrogen at a heating rate of 20 °C/min. Differential scanning calorimetry (DSC) analysis was made on a TA DSC Q10 instrument at a scan rate of 20 °C/min. Electrochemical measurements were made with EG&G Princeton Applied Research Model 273 Electrochemical Workstation. Redox potentials of the polymers were measured by cyclic voltammetry (CV) in acetonitrile containing 0.1 M tetrabutylammonium hexafluorophosphate as a supporting electrolyte, An Pt disk working electrode coated with polymer film, saturated calomel electrode (SCE) reference electrode, and Pt wire counter electrode were employed. MALDI-TOF mass spectrometric measurements were performed on Bruker Autoflex Ⅲ. All AFM measurements were performed using a Digital Instruments EnviroScope in tapping mode.

S2. Synthesis Procedures

4,7-Bis-(4-hexylthiophen-2-yl)benzo[1,2,5]thiadiazole (**DTBT**),[1] (2,5-dibromothiophen-3-ylmethyl)phosphonic acid diethyl ester,[2] and bis(trimethylstannane) derivative of BDT (**M2**)[3] were synthesized according to the procedure reported in the literatures.

Synthesis of DTBT-CHO

To a solution of **DTBT** (2.4 g, 5.1 mmol) in dichloroethane (25 mL) and anhydrous DMF (0.4 mL, 5.1 mmol) was added dropwise under nitrogen atmosphere, then $POCl_3$ (0.48 mL, 5.1 mmol) was added slowly. The mixture was stirred at 85 °C for 12 h. 30 mL water was added to quench the reaction. The mixture was extracted with CH_2Cl_2. After the solvent was removed, the crude product was purified using silica gel column chromatography (eluent: petroleum ether/dichloromethane = 1:1) to give 1.78 g of **DTBT-CHO** as an orange solid (Yield: 71%). ^1H NMR (400 MHz, $CDCl_3$): δ 10.12 (s, 1H), 8.07 (d, 2H, $J = 9.60$ Hz), 7.99 (d, 1H, $J = 7.64$, Hz), 7.89 (d, 1H, $J = 7.60$ Hz), 7.11

(s, 1H), 3.06 (t, 2H, *J* = 7.66 Hz), 2.72 (t, 2H, *J* = 7.62 Hz), 1.72-1.83 (m, 4H), 1.36-1.44 (m, 12H), 0.96 (m, 6H).

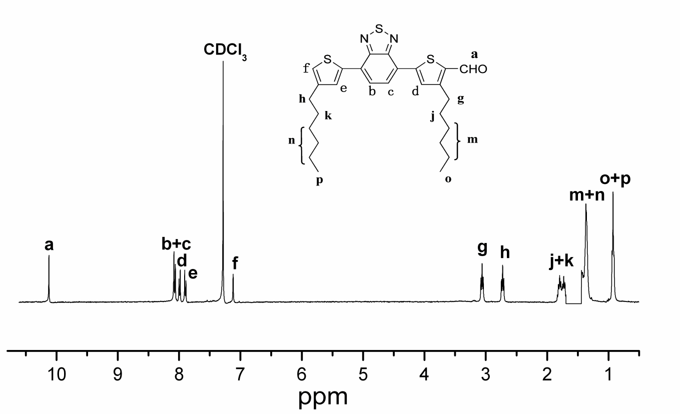

Fig. S1 ^{1}H NMR spectrum of **DTBT-CHO**.

Synthesis of M1

DTBT-CHO (0.497 g, 1 mmol) and (2, 5-dibromothiophen-3-ylmethyl)phosphonic acid diethyl ester (0.390 g, 1 mmol) were dissolved in THF (20 mL) and the solution was stirred at room temperature for 30 min under nitrogen atmosphere. Then potassium tertbutoxide (0.130 g, 1.15 mmol) was dissolved in THF (20 mL) and added dropwise to the solution. The reaction mixture was stirred for 5 h at room temperature, and then heated to 50 °C reflux for 12 h. After cooling to room temperature, the reaction mixture was extracted with dichloromethane and washed with dilute aqueous HCl solution. The organic phase was dried over anhydrous $MgSO_4$, and then the solvent was removed by rotary evaporation. The crude product was purified using silica gel column chromatography (eluent: petroleum ether/dichloromethane = 3:1) to give 0.48 g of **M1** as a light red solid (Yield: 65%). ^{1}H NMR (400 MHz, $CDCl_3$): δ 8.01 (s, 1H), 7.98 (s, 1H), 7.86 (d, 2H, *J* = 1.44 Hz), 7.86 (s, 1H), 7.22 (s, 1H), 7.12 (d, 1H, *J* = 15.96 Hz), 7.07 (s, 1H), 6.90 (d, 1H, *J* = 15.96 Hz), 2.70 (m, 4H), 1.71-1.72 (m, 4H), 1.36-1.42 (m, 12H), 0.92-0.93 (m, 6H). Elem. Anal. Calcd. for $C_{32}H_{34}Br_2N_2S_4$: C, 52.31%; H, 4.66%; N, 3.81%; S, 17.46%. Found: C, 53.26%; H, 5.19%; N, 3.80; S, 17.31%. MALDI-TOF MS ($C_{32}H_{34}Br_2N_2S_4$) m/z: calcd for 734.000; found 733.905.

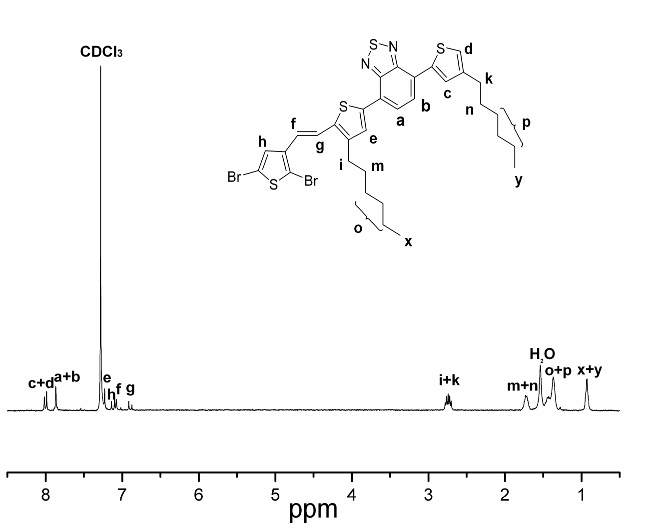

Fig. S2 ^{1}H NMR spectrum of **M1**.

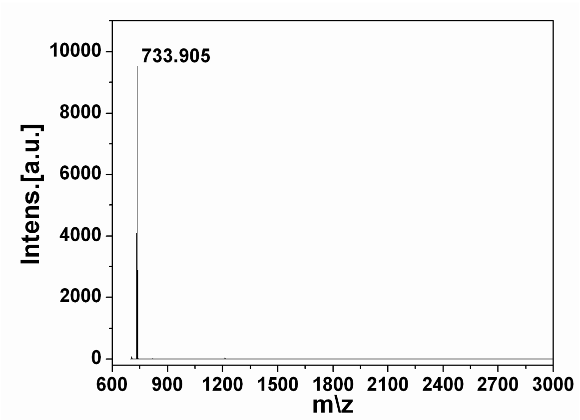

Fig. S3 MALDI-TOF mass spectrum of **M1.**

Synthesis of PTG1

To a 50 mL three-neck round bottom flask, **M1** (0.1835 g, 0.25 mmol), **M2** (0.193 g, 0.25 mmol), and dry toluene (20 mL) were added. The mixture was deoxygenated with nitrogen for 30 min. Then, $Pd(PPh_3)_4$ (50 mg, 33.75 mmol) was added under nitrogen and the reaction mixture was reacted for 72 h at 100 °C. After cooled to room temperature, the mixture was poured into methanol (200 mL). A purple-red precipitate was collected by filtration. The product was purified by washing with methanol and hexane in a Soxhlet extractor for 24 h each. It was extracted with hot chloroform in an extractor for 24 h. After removing solvent, a purple-red solid was collected (0.2 g, 78.4%). ^{1}H NMR (400 MHz, $CDCl_3$): δ 7.12-8.08 (br, 8H), 4.23-4.26 (br, 4H), 2.63-2.67 (br, 4H), 0.94-1.37 (br, 52H). ^{13}C NMR (100 MHz, $CDCl_3$): δ 144.25, 128.96, 128.78, 125.32, 121.56, 68.18, 40.79, 31.69, 30.54, 29.65, 29.35, 29.05, 28.73, 23.95, 23.21, 22.61, 14.18, 14.04, 11.47, 0.97. Anal. Calcd. for $(C_{58}H_{70}N_2O_2S_6)_n$: C, 68.32%; H, 6.92%; N, 2.75%; S, 18.87%. Found: C, 67.73%; H, 7.79%; N, 2.63; S, 19.08%.

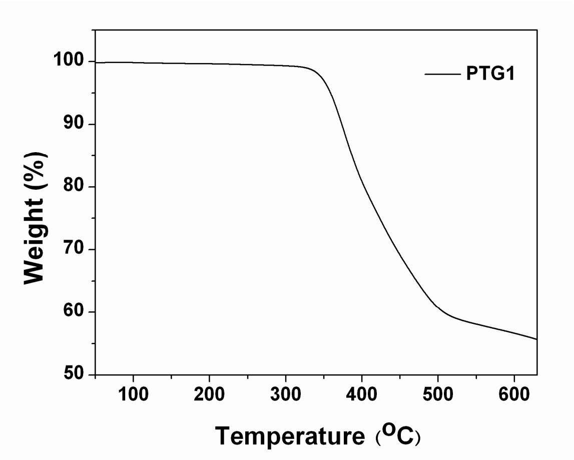

Fig. S4 TGA curve of **PTG1** collected under N_2 at a heating rate of 20 °C/min.

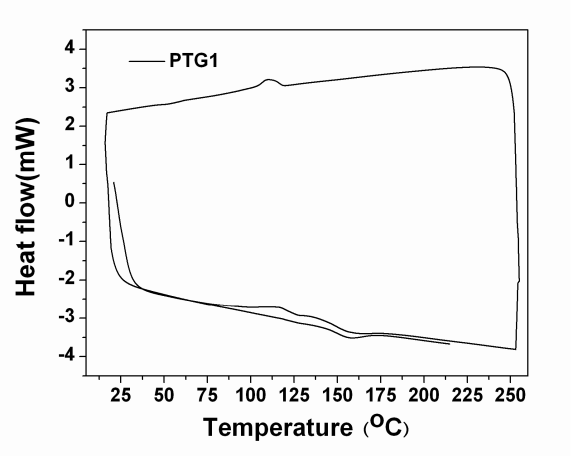

Fig. S5 DSC curve (1st heating, cooling scan and 2nd heating) of **PTG1** collected at a scan rate of 20 °C/min.

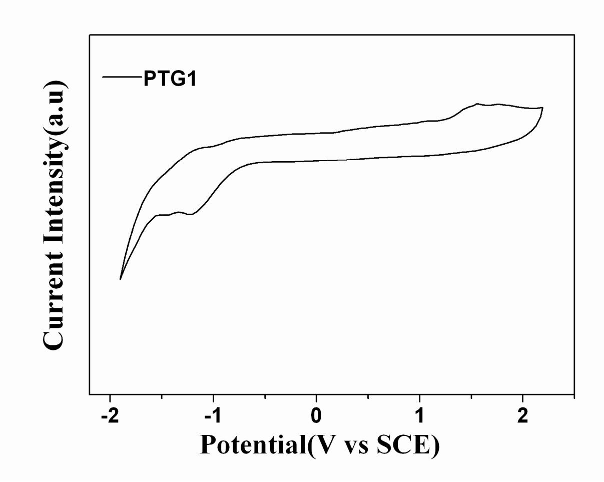

Fig. S6 CV curve of **PTG1** on a Pt disk in 0.1 mol/L Bu_4NPF_6 acetonitrile solution.

S3. PSC Device Fabrication and Characterization

The BHJ solar cells were prepared on pre-patterned commercial ITO glass substrates. The thickness and sheet resistance of the ITO are 120 nm and 12 Ω/square, respectively. The active area of each solar cell device is 0.5 cm^2. The substrates were sonicated sequentially in detergent, DI water, acetone, and isopropanol. Immediately prior to device fabrication, the substrates were treated in a UV-ozone oven for 15 min. First, a poly(3,4-ethylenedioxythiophene)-poly(styrene sulfonate) (PEDOT-PSS) thin film (30 nm) was spin-coated and then baked at 140 °C for 15 min. Secondly, an active layer (80 or 90 nm) was spin-coated on top of the PEDOT-PSS from the a solution of chlorobenzene (CB) of the polymer:$PC_{71}BM$ blends (ADS) (1:1 weight ratio). In the case of the devices using a processing additive, 1,8-diiodooctane (3% by volume) was added to the solutions before use. Finally, 5 nm of BCP and 80 nm of Al were deposited on the top of the active layer in a vacuum of $2\text{-}8 \times 10^{-7}$ Torr to complete the photovoltaic device fabrication.

The current-voltage (*J*-*V*) characteristics and PCE were measured with a Keithley 2400 Digital Source Meter under air mass 1.5 global (AM 1.5G) irradiation of 100 mW/cm^2 (ScienceTech 150W solar simulator with an AM 1.5G filter) at room temperature in a nitrogen filled glove-box. The light intensity was calibrated with a power meter (Gentec Inc., UP19K-30H-H5). After the *J*-*V* measurement, the sample was exposed in air for the external quantum efficiency (EQE) and reflectance measurements.

The EQE measurement was performed using a Jobin-Yvon Triax 180 spectrometer, a Xenon light source, a Merlin lock-in amplifier, a calibrated Si detector, and an SR570 low noise current amplifier. The film thicknesses were measured by a Dektak profilometer. The reflectance data were collected at 6 degree using a Lambda 950 UV-vis-NIR spectrometer. The average performance parameters of the test cells were summarized in Table S1. Reported values are an average of four devices.

Device Structure:

A) ITO / PEDOT (30 nm) / **PTG1**:$PC_{70}BM$ (1:1, CB, 90 nm)/ BCP / LiF / Al
B) ITO / PEDOT (30 nm) / **PTG1**:$PC_{70}BM$ (1:1, CB, 80 nm)/ BCP / LiF / Al
C) ITO / PEDOT (30 nm) / **PTG1**:$PC_{70}BM$ (1:1, CB w/ 3% DIO, 90 nm)/ BCP / LiF / Al
D) ITO / PEDOT (30 nm) / **PTG1**:$PC_{70}BM$ (1:1, CB w/ 3% DIO, 80 nm)/ BCP / LiF / Al

Table S1. Device parameters and EQE-calibrated J_{EQE} and $\mathrm{PCE}_{\mathrm{EQE}}$ values of the test devices.

Devices	J_{sc} [mA/cm^2]	J_{EQE} [mA/cm^2]	V_{oc} [V]	FF	$\mathrm{PCE}_{\mathrm{JV}}$ [%]	$\mathrm{PCE}_{\mathrm{EQE}}$ [%]
A	7.67±0.49	6.92	0.88	0.42	2.82±0.18	2.55
B	7.80±0.41	7.33	0.88	0.42	2.92±0.15	2.74
C	8.32±0.53	8.10	0.86	0.45	3.24±0.21	3.16
D	9.95±0.64	8.33	0.84	0.49	4.06±0.26	3.40

Slightly lower J_{EQE}, as compared to the corresponding J_{sc}, was observed for all test cells. This is caused by the spectral mismatch of the emission from solar simulator and the standard AM 1.5G spectrum. However, the error between the J_{EQE} and the J_{sc} is less than 10% for all the tested devices except for device D.

For all devices we tested, the fill factors (FF) were in the range of 0.42–0.49, which are comparably lower than those reported for the best PSCs (FF ~ 0.65–0.70).[4] One of the possible reasons for the low FF may be due to the high charge recombination rate, which can be attributed to the non-ideal phase separation. Another possible reason is due to the field-dependence of exciton dissociation rate. If the exciton dissociation rate is strongly dependent on the internal field strength, the FF will also be significantly reduced. Further optimization of the morphology may lead to even higher performance.

S4. FET Device Fabrication and Characterization

The hole mobility of **PTG1** was measured on organic field-effect transistors (FETs) with a bottom-contact structure. Gold source and drain electrodes were sputtered on the SiO_2/Si substrate prior to the deposition of the polymer film. The channel width and length of the transistors are 10 mm and 20 μm, respectively. The polymer thin films were spin-coated on the SiO_2/Si substrates from the chlorobenzene solution to cover the source and drain electrodes. The OFETs were characterized inside a dark box at room temperature and under nitrogen with an Agilent (4155c) semiconductor parameter analyser. The hole mobilities were calculated in the saturation regime using the following equation $I_{DS} = (W/2L)\mu C_i(V_G-V_T)^2$, where I_{DS} is the source-drain current, W and L are, respectively, the channel width and length, μ is the field-effect mobility, Ci is the capacitance per unit area of the SiO_2 layer, and V_G and V_T are, respectively, the gate voltage and threshold voltage.

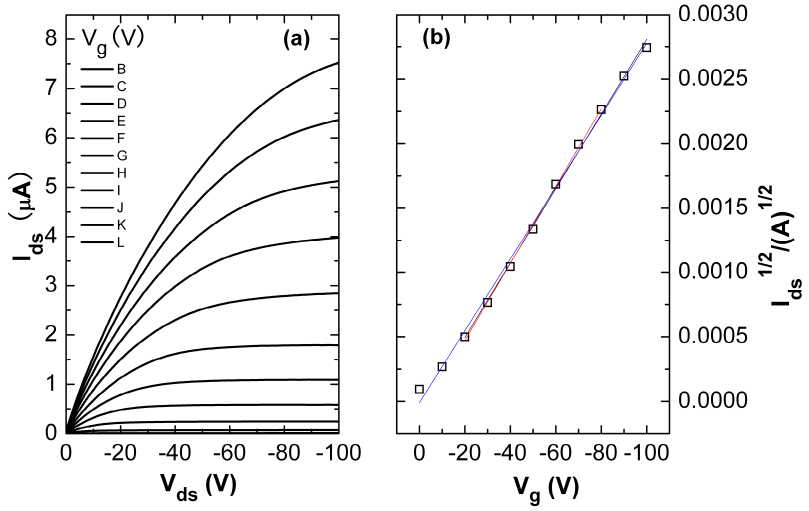

Fig. S7 (a) Output characteristics at various gate biases V_g and (b) square-root of the drain current of the transfer characteristics for **PTG1** FET.

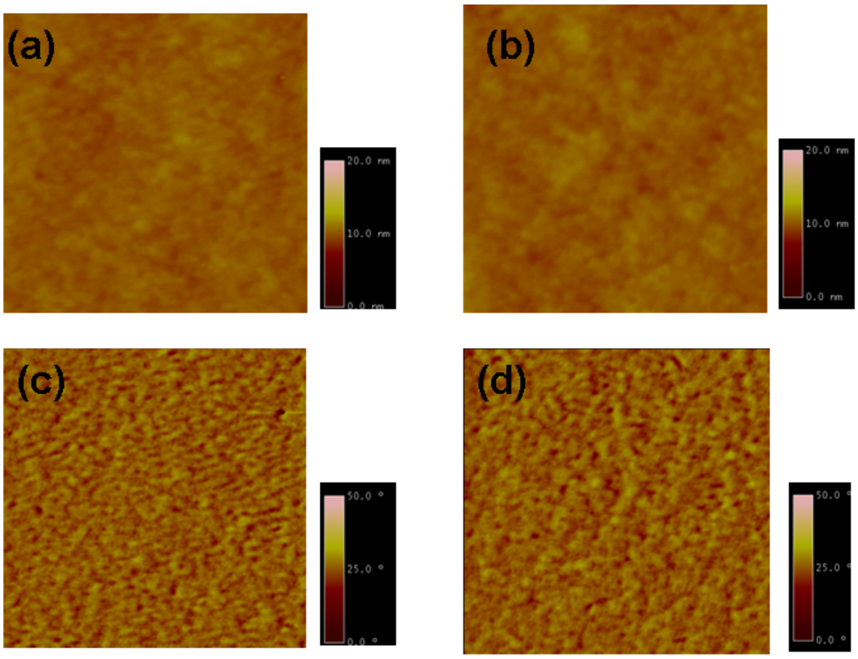

Fig. S8 AFM Morphology and of the active layer in (a) Device B (w/o DIO) and (b) Device D (w/ DIO); AFM phase images of the active layer in (c) Device B (w/o DIO) and (d) Device D (w/ DIO). The size of images is 500 nm × 500 nm.

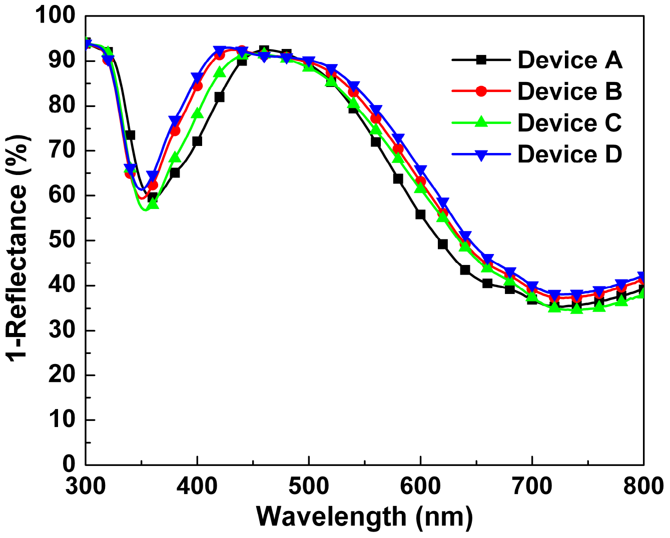

Fig. S9 Total absorption (1-reflectance) spectra of the **PTG1**-based four photovoltaic devices A–D.

S5. References

1. S. Zhang, Y. Guo, H. Fan, Y. Liu, H. Chen, G. Yang, X. Zhan, Y. Liu, Y. Li and Y. Yang, *J. Polym. Sci., Part A: Polym. Chem.*, 2009, **47**, 5498.

2. J. Hou, L. Huo, C. He, C. Yang and Li, Y. *Macromolecules*, 2006, **39**, 594.

3. Y. Liang, Y. Wu, D. Feng, S.-T. Tsai, H.-J. Son, G. Li and L. Yu, *J. Am. Chem. Soc.*, 2009, **131**, 56.

4. M. S. Kim, M. G. Kang, L. J. Guo and J. Kim, *Applied Physics Letters*, 2008, **92**, 133301.